Biomedicine & Pharmacotherapy 88 (2017) 667–676

Available online at
ScienceDirect
www.sciencedirect.com

Elsevier Masson France
EM|consulte
www.em-consulte.com/en

Gold coated poly (ε-caprolactonediol) based polyurethane nanofibers for controlled release of temozolomide

Mohammad Irani[a], Gity Mir Mohamad Sadeghi[b,*], Ismaeil Haririan[c]

[a] Department of Chemical Engineering, Amirkabir University of Technology, Tehran, Iran
[b] Department of Polymer Engineering and Color Technology, Amirkabir University of Technology, P.O. Box 15875/4413, Tehran, Iran
[c] Department of Pharmaceutical Biomaterials and Medical Biomaterials Research Center, Faculty of Pharmacy, Tehran University of Medical Sciences, Tehran, Iran

ARTICLE INFO

Article history:
Received 27 December 2016
Received in revised form 15 January 2017
Accepted 16 January 2017

Keywords:
Polyurethane
Nanofiber
Gold
Temozolomide
Controlled release

ABSTRACT

In the present study, the temozolomide (TMZ) loaded poly (ε-caprolactonediol) based polyurethane (PCL-Diol-b-PU) nanofibers were fabricated as local delivery systems against glioblastoma. The structure and morphology of nanofibers were characterized using FTIR and SEM analysis. The gold nanoparticles were coated on the nanofibers surface to enhance the efficacy of nanofibers for local chemotherapy of brain tumors. The effect of various ratios of DMF/THF solvents and solution concentration on the morphology and fiber diameter of PCL-Diol-b-PU nanofibers was investigated. The small burst release of TMZ with sustained TMZ release from both PCL-Diol-b-PU and gold-coated PCL-Diol-b-PU nanofibers were achieved over 30 days. The Korsmayer-Peppas kinetic and Fickian diffusion models were used to describe the mechanism of TMZ release from nanofibers. The in vitro cell viability results revealed that the higher antitumor activity of synthesized nanofibers against glioblastoma cells compared with pristine TMZ. It was concluded that the prepared nanofibrous implants showed a higher potential in the local chemotherapy of brain tumors.

1. Introduction

The drug delivery into the brain due to the presence of blood-barrier brain is limited.

The presence of the blood-barrier brain, the blood–cerebrospinal fluid barrier and the blood–tumor barrier significantly reduces the therapy efficiency of brain tumors [1]. These barriers prevent the penetration of drug into the central nervous system neoplasms. Therefore, the development of new delivery systems is necessary for achieving the high intra-tumoral drug concentrations, and following the controlled release of drug for improvement of the efficacy of drug in patients.

The predetermined amount of drug delivery over a specified period of time is the main role of the controlled release of drug for increasing the efficiency of drug therapy as well as reducing the toxic side effects of the drug. The direct administration of drugs into the brain parenchyma in which drug-loaded delivery systems was implanted into brain tumors, resulted in a better controlled drug release. Several brain drug delivery systems in the forms of nanoparticles, catheters, wafers, micro/nanoparticles and electrospun nanofibers have been used for controlled release of drugs into the brain tumor cells [2]. The obtained results have proven that the controlled and sustained release of drugs into the brain tumors can be achieved by the nanafibrous delivery systems [2].The higher surface area and fine pores of nanofibers prepared by the electrospinning process resulted in the higher drug encapsulation efficiency compared to other drug formulations [3]. In recent years, the anticancer drugs such as Paclitaxel, doxorubicin hydrochloride, daunorubicin and temozolomide (TMZ) have been incorporated into the natural and synthetic polymeric nanofibers including chitosan [3,4], poly-(D,L-lactide-co-glycolide) [2,5], polypropylene carbonate [6], poly(L-lactic acid) [7–13], poly(ethylene glycol) – poly(L-lactic acid) [14] and polyurethane (PU) [15] for sustained drug delivery systems in the local chemotherapy of cancers. Xie et al. [2] fabricated the poly-(D,L-lactide-co-glycolide) nanofibers as an implant for the sustained delivery of paclitaxel as an anticancer drug to treat C6 glioma. Xu et al. [14] incorporated the paclitaxel and doxorubicin hydrochloride drugs into the poly (ethylene glycol)– poly(L-lactic acid) nanofibers for antitumor activity against Glioma C6 cells. Xie et al. [16] fabricated the cisplatin-loaded poly(L-lactic acid) fibers for sustained delivery of cisplatin to treat C6 glioma. Ranganath and Wang [17] prepared the

* Corresponding author.
E-mail address: gsadeghi@aut.ac.ir (G. Mir Mohamad Sadeghi).

http://dx.doi.org/10.1016/j.biopha.2017.01.097
0753-3322/

paclitaxel-loaded biodegradable poly-(D,L-lactide-co-glycolide) microfibrous implant against malignant glioma. Rao et al. [18] studied the influence of aligned core-shell electrospun nanofibers migration of malignant brain tumors. Guo et al. [19] developed the implantable curcumin-loaded poly(3-caprolactone)-poly(ethylene glycol)-poly(3-caprolactone) nanofibers by the electrospinning method for postoperative therapy of glioma tumors.

Due to very high interstitial pressure in the brain/tumor, PUs nanofibers with their excellent physical properties, higher stability and biocompatibility can be used as a good candidate for local delivery of anticancer drugs into the brain. Also, Reddy et al. proved that the regulated release rate and transport mode of drug release have been provided by segmented polyurethane hydrogels [20]. However, there is no study about the application of segmented polyurethane nanofibers as an implant device for local drug delivery. Among anticancer drugs, TMZ is the current standard-of-care chemotherapeutic in the treatment of glioblastoma [21]. Gliomas are the most common primary brain tumors in adults. However, due to its short plasma half-life of 1.8 h and poor stability of TMZ, the use of pristine TMZ is limited. In recent studies, TMZ has been encapsulated into the polymeric micro/nano particles to improve the solubility and stability as well as its controlled release into the brain tumors [22–24]. However, there is a dearth of literature on the encapsulation of TMZ into the nanofibers.

In recent years, nanometer-scale particles such as gold nanoparticles have been successfully used in cancer therapy. Huo et al. [25] indicated that the gold-coated tiopronin with the average size of 50 nm penetrated more deeply into the breast tumors compared to pristine tiopronin.

The gold nanoparticles due to the small size, and low toxicity have a high potential across the blood-barrier brain. Joh et al. [26] indicated that the gold nanoparticles increased cellular DNA damage inflicted by ionizing radiation in human glioblastoma −derived cell lines and enhanced the selective targeting of brain tumors. They introduced a novel strategy for enhancing the efficacy of nanoparticle agents against brain tumors such as glioblastoma. Dhar et al. [27] demonstrated that the doxorubicin hydrochloride −conjugated gold nanoparticles could lower the effective dose administered to patients during the brain tumor treatment with the higher transport of drugs across the blood-barrier brain. However, there is no study about gold coated nanofibers for brain tumor treatment.

In the present study, the poly (ε-caprolactonediol) based polyurethane (PCL-Diol-b-PU) was synthesized and the nanofibers of PCL-Diol-b-PU were fabricated via the electrospinning process. The influence of solvent type and solution concentration on the morphology of PCL-Diol-b-PU nanofibers was investigated to obtain uniform nanofibers. TMZ as an anticancer drug has been encapsulated into the PCL-Diol-b-PU nanofibers. The gold nanoparticles were also synthesized and coated on the surface of drug loaded- PCL-Diol-b-PU nanofibers. Drug loading efficiency and in vitro drug release of TMZ loaded- PCL-Diol-b-PU nanofibers and gold-coated PCL-Diol-b-PU nanofibers containing TMZ have been evaluated. The antitumor activity of synthesized TMZ loaded nanofibers was also investigated on the glioma cell lines.

2. Experimental

2.1. Material

Hexamethylenediisocyanate, 1,4-Butanediol, *N,N*-Dimethylformamide (DMF) and Tetrahydrofuran(THF) were provided from Merck (Merck, Germany). Polycaprolactonediol (PCL-Diol, $M_w = 2000\ g\ mol^{-1}$), phosphate buffer saline (PBS, pH:7.4), $HAuCl_4$, sodium citrate and temozolomide were purchased from Sigma-Aldrich (Aldrich, Germany). Deionized water was used throughout this work.

2.2. Synthesis of PCL-Diol-b-PU

The PCL-Diol-b-PU was synthesized using a method as described previously [28]. Briefly, 12 g PCL-Diol was reacted with 3.02 g hexamethylenediisocyanate in a glass vial reactor at 85 °C for 3 h. Then 1.08 g 1,4-Butanediol was added to the reactor content and the reaction was continued for a further 30 min. Finally, the reactor contents were derided in a vacuum oven at 70 °C for 24 h. The synthesized PCL-Diol-b-PU were washed three times with deionized water.

2.3. Electrospinning process

The synthesized PCL-Diol-b-PU (7, 10 and 15 wt.%) was dissolved in DMF/THF mixed solvents with various ratios of DMF/THF (10/0, 8/2, 5/5, 2/8 and 0/10 V/V) under stirring at 60 °C for 6 h. The prepared solution was placed in a 5 mL plastic syringe equipped with a syringe needle (19 gauge nozzle). The high voltage of 19 kV was applied between the needle and collector (tip-collector distance of 12 cm) to produce the PCL-Diol-b-PU nanofibers. The flow rate of the solution and speed collector through the electrospinning process were 1 mL/h and 1000 rpm, respectively. For loading TMZ into the PCL-Diol-b-PU/Au nanofibers, 10, 20 and 40 mg TMZ were dispersed into the solution under stirring for further 4 h before electrospinning process. The set-up of the electrospinning process was provided from Nanomeghyas Company (Iran).

2.4. Synthesis of gold nanoparticles and coating on the PCL-Diol-b-PU nanofibers

The gold nanoparticles were synthesized by citrate reduction of $HAuCl_4$, as described previously [29]. Briefly, 100 mL of 1 mM $HAuCl_4$ was refluxed for 10 min. Then 10 mL of 38.8 mM sodium citrate solution at 60 °C was added into the $HAuCl_4$ solution and the reflux was continued for a further 30 min to obtain the red solution of gold nanoparticles. The gold nanoparticles solution was filtered using a 0.2 μm pore size nylon filter system (Millipore).

For coating of gold nanoparticles on the surface of nanofibers, the fabricated PCL-Diol-b-PU nanofibers were poured into 20 mL of 50 and 200 $\mu g\ mL^{-1}$ gold nanoparticles suspensions at room temperature for 12 h. Then, the gold-coated nanofibers were washed with water to remove the excess gold nanoparticles on the surface of nanofibers.

2.5. Characterization tests

The functional groups of synthesized nanofibers were determined using Fourier transform infrared spectrometer (FTIR, Equinox 55 FTIR spectrometer) spectra in the range of 400–4000 cm^{-1}. The morphology of nanofibers was characterized using scanning electron microscopy (SEM, JEOL JSM-6380) after gold coating. The diameter distribution of the nanofibers was obtained by an image analyzer (Image-Proplus, Media Cybernetics). Transmission electron microscopy (TEM, Philips), UV–vis spectroscopy (JAS·CO V-530, Japan) and an atomic absorption spectrophotometer (AAS, Varian SpectrAA-300, Varian, California) were used to characterize the synthesized gold nanoparticles. The quantification of the TMZ was carried out using UV–vis spectrophotometer at λ_{max} of 255 nm. Viscosities of PCL-Diol-b-PU solutions were measured using the Ubbelohde I capillary viscometer.

2.6. Drug loading efficiency

To determine the drug loading efficiency, the prepared nanofibers containing 10, 20 and 40 mg TMZ were degraded by dissolving in DMF/THF for 4 h and the final concentration of the drug was measured using UV–vis spectrophotometer. The drug loading efficiency (DLE, %) was calculated as follows:

$$DLE(\%) = \frac{Actual\ drug\ content}{Drug\ loading\ content\ at\ the\ beginning} \times 100\% \quad (1)$$

2.7. In vitro drug release and drug release mechanism

The drug release from TMZ-loaded PCL-Diol-b-PU nanofibers was investigated at 37 °C in a pH of 7.4. Briefly, 20 mg of TMZ-loaded PCL-Diol-b-PU nanofibers were transferred to a dialysis tube with a molecular weight cut off of 12 000−14 000. The dialysis tube was immersed into 20 mL of 0.05 M phosphate buffered saline (PBS, pH 7.4). The suspensions were placed in a shaking water bath (Hidolff) under stirring for 30 days. To determine the amount of TMZ released, 2 mL released solution were taken from the dissolution medium at desired time intervals (1, 3, 6, 12, 24, 48, 72, 96, 120, 168, 240, 336, 408, 504, 672 and 720 h); while an equal amount of fresh PBS was added back to the incubation media. The release experiments were conducted in triplicate, and the average data were reported.

The drug release mechanism was investigated using the Korsmayer-Peppas equation as follows:

$$\frac{M_t}{M_0} = kt^n \quad (2)$$

where M_t/M_0 is the drug fraction released at time t, K is a constant characteristic of the drug–polymer system and n is the diffusional coefficient related to the release mechanism [30]. When $n < 0.5$, a Fickian diffusion controlled-release is implied; while $0.5 < n < 1.0$ indicates a release non-Fickian and 1 stands for zero order (case II transport). When n value is greater than 1.0, it indicates super case II transport.

2.8. Diffusion coefficients

The apparent diffusion coefficient of a nanofibrous matrix can be calculated by means of a 1D unsteady state form of the Fick's second law of diffusion [31] as follows:

$$\frac{M_t}{M_\infty} = \left(\frac{16 D_{app} t}{\pi h^2}\right)^{0.5} \quad (3)$$

where M_t and M_∞ are the cumulative mass of the diffusing TMZ released from the nanofibers after t and infinite time (∞), respectively. D_{app} is the apparent diffusion coefficient of the system and h is the thickness of the fibers (about 20 μm). The Korsmayer-Peppas parameters and diffusion coefficients were obtained by non-linear regression using MATLAB software.

2.9. Degradation behavior of nanofibers

The degradation rate of nanofibers was investigated by immersion of 50 mg nanofibers in 20.0 mL of PBS. At desired time intervals, the nanofibrous samples were covered and washed with water to remove residual buffer salts, and dried in a vacuum oven at 70 °C for 24 h. The mass loss was determined by comparing the dry weight remaining at time t with the initial weight. Triplicate samples for each kind of nanofibers were used and the average values were reported.

2.10. Cell culture and cell viability

U-87 MG human glioblastoma cell lines provided by the Pasteur Institute of Iran (IPI, Tehran, Iran) were cultured in RPMI with 10% fetal calf serum and 1% penicillin-streptomycin at 37 °C in a humidified atmosphere of 5% CO_2. Cells were detached with 0.25% trypsin-EDTA for cytotoxicity analysis.

The cell viability test was determined using a colorimetric 3-(4,5- dimethylthiazol-2-yl)-2,5-diphenyltetrazolium bromide, a tetrazole (MTT) assay as previously described [31,32]. Briefly, 3×10^4 cells were seeded within 96-well plates. The cells were incubated at 37 °C and 5% CO_2 for 24 h. After 24 h incubation, the prepared TMZ, PCL-Diol-b-PU/TMZ (20 mg) nanofibers and gold-coated-PCL-Diol-b-PU/TMZ (20 mg) nanofibers were prepared with 1% DMSO and treated to the cells at the designated time points.1% DMSO was used as negative control. Finally, the extraction solution of nanofibers was removed and replaced with 100 μL/well MTT solution and re-incubated for a further 4 h. After treating the cells with Sorenson buffer (MBRC, Tehran, Iran), the optical density of each well was read using a microplate reader (Multiskan MK3, Thermo Electron Corporation, USA) at a wavelength of 570 nm, and growth inhibition was calculated.

3. Results and discussion

3.1. Characterization of gold nanoparticles

The TEM image of synthesized gold nanoparticles is illustrated in Fig. 1. As shown, the uniform nanoparticles with narrow size distribution sizes in the range of 15 to 25 nm and average particle size of 18 nm were synthesized. The optical absorption spectra of gold nanoparticles is illustrated in Fig. 1b. As shown, the gold nanoparticles were successfully synthesized with the maximum adsorption peak at 525 nm.

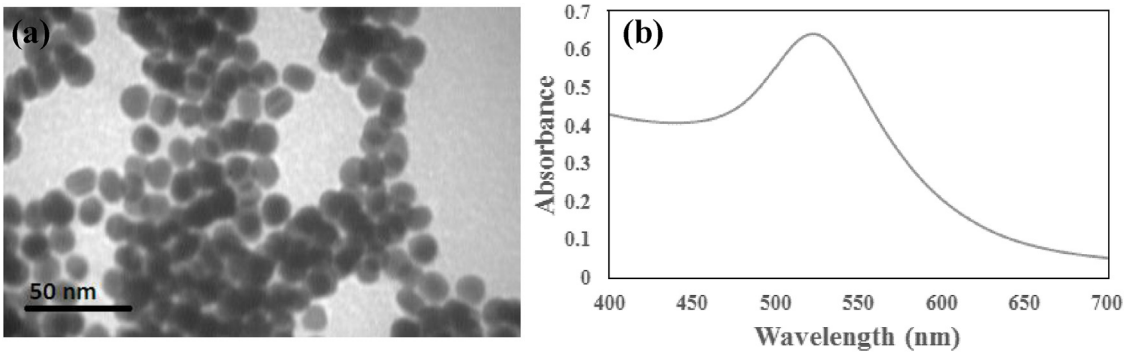

Fig. 1. (a) TEM image and (b) UV–vis spectra of gold nanoparticles.

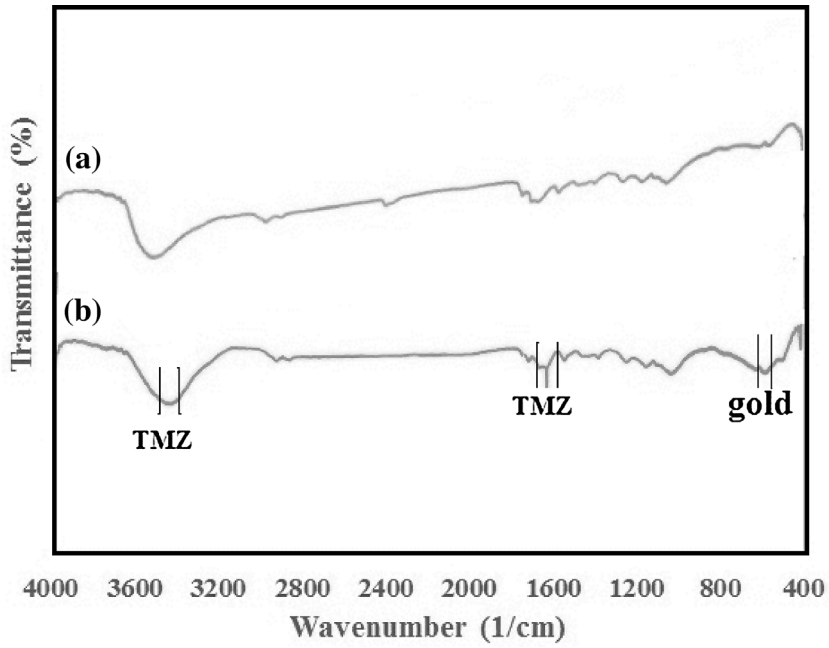

Fig. 2. FTIR spectra of (a) PCL-Diol-b-PU nanofibers and (b) gold-coated PCL-Diol-b-PU/TMZ nanofibers.

3.2. Characterization of nanofibers

3.2.1. FTIR analysis

The FTIR spectra of PCL-Diol-b-PU nanofibers and gold-coated PCL-Diol-b-PU/TMZ nanofibers are illustrated in Fig. 2. As shown, bands at 2924 and 2848 cm^{-1} are assigned to the asymmetrical and symmetrical —CH_2 stretching, respectively. The —OH and —N=C=O absorption bands of the PCL diol and hexamethylene-diisocyanate are observed at 3433 and 2239 cm^{-1}, respectively. The other main functional groups of PCL-Diol-b-PU nanofibers are the NH stretching at 3400–3600 cm^{-1}, the non-hydrogen bonded —C=O stretching at 1720 cm^{-1}, the NH bending vibration at 1553 cm^{-1} and the C—O band at 1250 cm^{-1} [28]. For gold-coated PCL-Diol-b-PU/TMZ nanofibers, two strong characteristic bands of TMZ at 1620 and 3400–3600 cm^{-1} are related to C=C or C=N stretching vibration and NH stretching, respectively [33]. The adsorption peak between 520 and 550 cm^{-1} could be attributed to the presence of gold nanoparticles on the surface of nanofibers [34].

3.2.2. SEM images

The influence of solution concentration and solvent type on the morphology of nanofibers is illustrated in Fig. 3. As shown, the 100% THF was not successful in preparation of PCL-Diol-b-PU nanofibers in various concentrations of PCL-Diol-b-PU solutions. It could be attributed to the faster evaporation of solvent at the

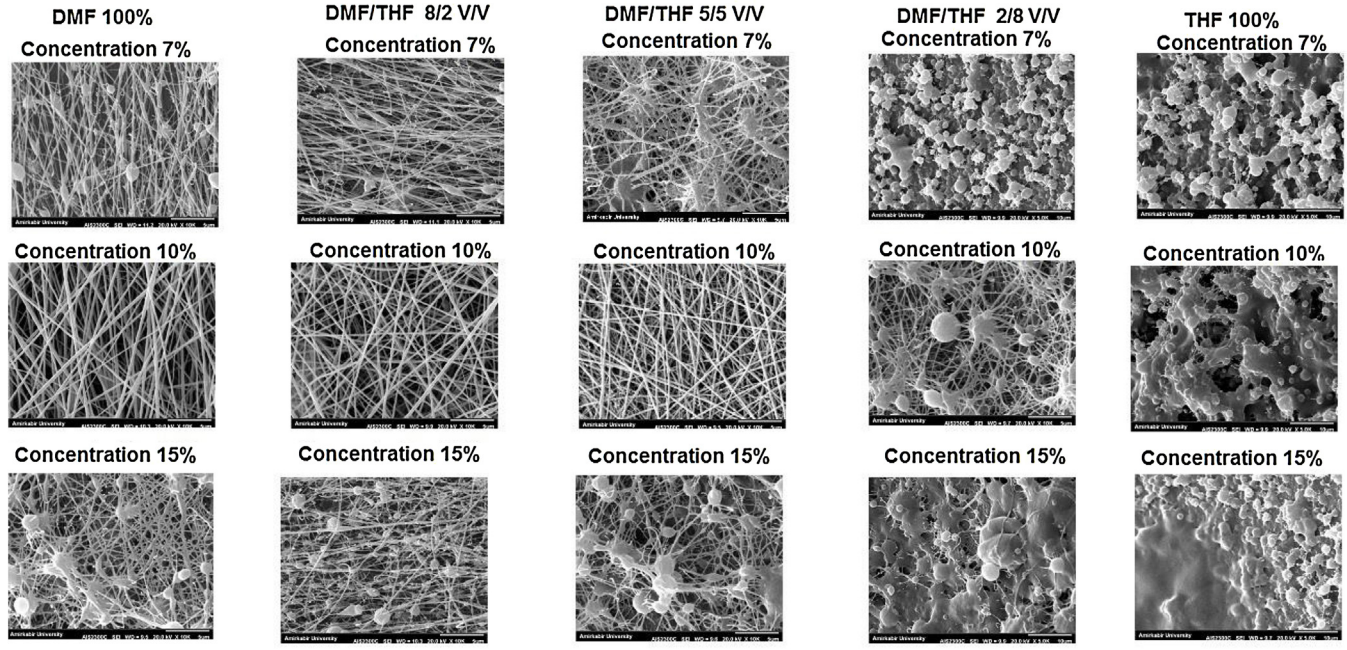

Fig. 3. SEM images of PCL-Diol-b-PU nanofibers in various volume of solvents and solution concentrations.

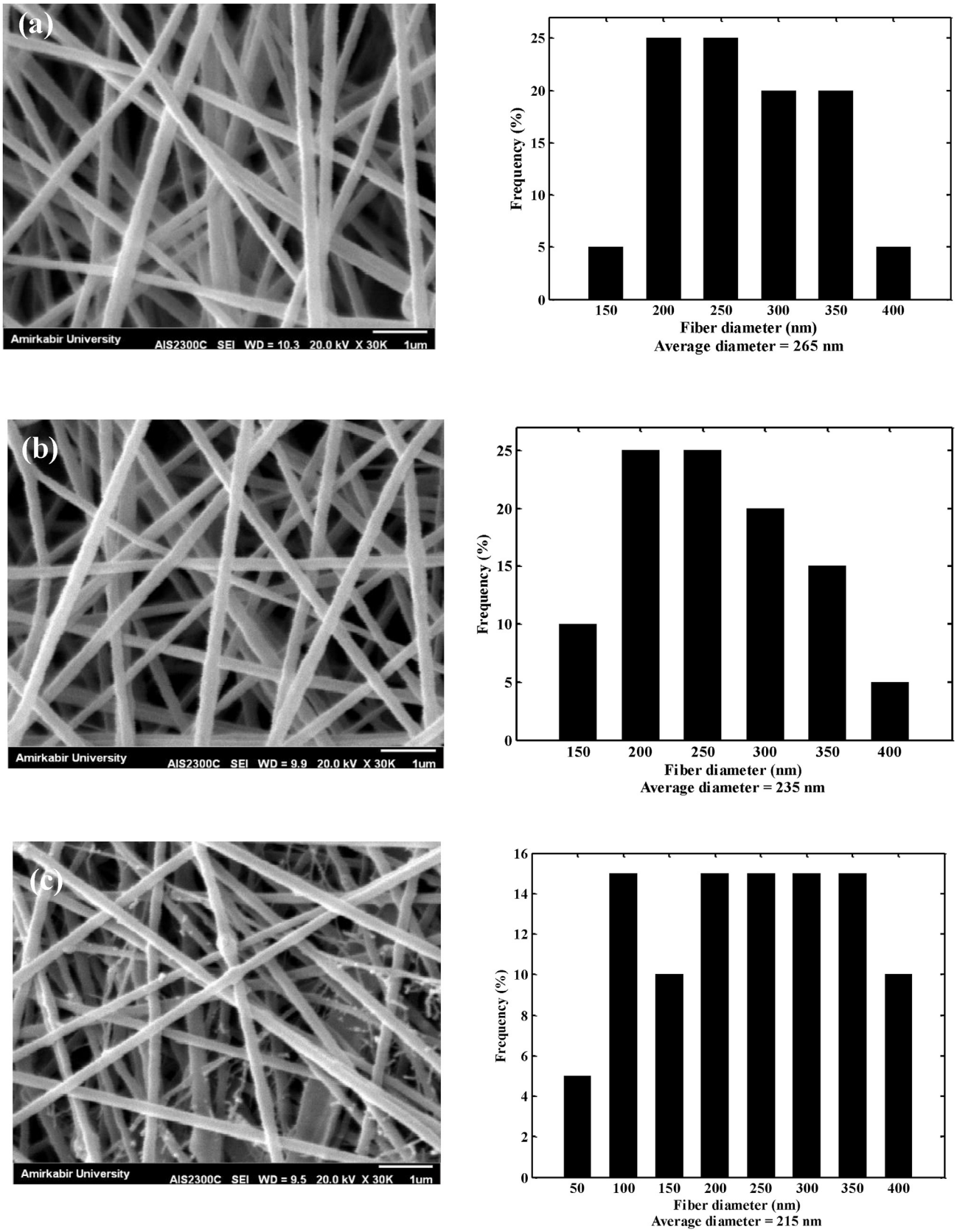

Fig. 4. SEM images and diameter distribution of 10% PCL-Diol-b-PU nanofibers with (a) DMF 100%, (b) DMF/THF 8/2 and (c) DMF/THF 5/5 ratios.

needle tip during the electrospinning process. A similar trend was obtained for PU nanofibers by Erdem et al. [35]. The beaded nanofibers were only produced in 10% solution concentration by mixing of the THF solvent with DMF in a ratio of 8/2. This could be attributed to the enhancement in viscosity of solution in which the solvent evaporation rate was decreased. The obtain results

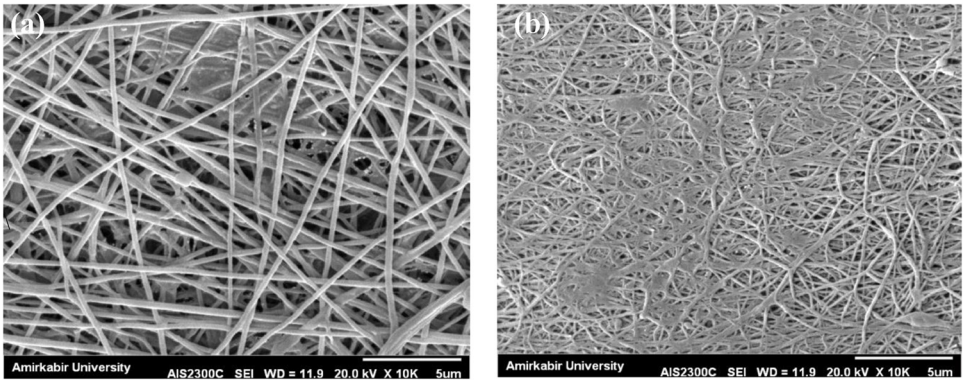

Fig. 5. SEM images of gold-coated PCL-Diol-b-PU nanofibers poured in 50 and 200 $\mu g\,mL^{-1}$ gold nanoparticles suspensions.

revealed that the 10% PCL-Diol-b-PU solution concentration was appropriate to produce the uniform PCL-Diol-b-PU nanofibers (η: 1.12 dl/g). The lower viscosity of 7% solution concentration (η: 0.79 dl/g) resulted in fabrication of beaded fibers by using different solvents. At higher concentration (15%), the solvent evaporation rate due to the higher viscosity of solution (η: 1.59 dl/g) was slower, which resulted in fabrication of fiber consisting droplets [36].

To determine the better morphology of fibers, a high resolution of nanofibers was chosen and SEM images and diameter distribution of nanofibers in a solution concentration of 10% by using different solvents (DMF 100%, DMF/THF 8/2 and DMF/THF 5/5) are illustrated in Fig. 4. As shown, the uniform nanofibers with average diameter of 265 nm were prepared by pure DMF (Fig. 4a). In another nanofibrous sample, by mixing THF with DMF solvent at a ratio of 8:2 DMF/THF, the solution viscosity was decreased and the affinity of solution for stretching was increased which resulted in the formation of thinner fibers with an average diameter of 235 nm (Fig. 4b). By increasing the THF ratio at DMF/THF 5:5, the surface tension, conductivity and viscosity of solution were increased and thinner fibers were produced. However, the uniformity of fibers was decreased and the fiber diameters were produced in a wide range (Fig. 4c). Therefore, the mixed solvent DMF/THF 8:2 and solution concentration of 10% due to the formation of the same fibers was chosen for further experiments.

The SEM images of gold-coated PCL-Diol-b-PU nanofibers are illustrated in Fig. 5. As shown, the gold nanoparticles were successfully coated on the nanofibers surfaces with 200 $\mu g\,mL^{-1}$ gold nanoparticles rather than 50 $\mu g\,mL^{-1}$ gold nanoparticle suspension. Based on AAS results, the gold content on the surface of nanofibers was found to be 8.24 and 23.8 $\mu g\,mL^{-1}$ for nanofibers poured in 50 and 200 $\mu g\,mL^{-1}$ gold nanoparticles suspensions.

To evaluate the effect of TMZ on the morphology of electrospun nanofibers, the SEM images of PCL-Diol-b-PU and TMZ loaded-PCL-Diol-b-PU nanofibers were compared. The results are illustrated in Fig. 6. As shown, the morphology and fiber diameter of nanofibers did not significantly change by incorporation of TMZ into the PCL-Diol-b-PU nanofibers, successfully. The average diameter of nanofibers before and after encapsulation of TMZ were found to be 235 and 250 nm, respectively.

3.3. Drug loading efficiency

The TMZ loading efficiency from nanofibers is illustrated in Table 1. As shown, a high capsulation efficiency of TMZ was observed for TMZ loaded PCL-Diol-b-PU nanofibers. This is while the loading efficiency of TMZ for gold-coated PCL-Diol-b-PU/TMZ nanofibers was significantly decreased. Decreases in TMZ encapsulation efficiency for gold-coated PCL-Diol-b-PU/TMZ nanofibrous formulations could be attributed to the TMZ release from nanofibers during gold coating.

3.4. In vitro release of TMZ and kinetic studies

The TMZ release behavior of PCL-Diol-b-PU nanofibers and gold-coated PCL-Diol-b-PU nanofibers consisting of different drug contents (10, 20 and 40 mg) are illustrated in Figs. 7 and 8. As shown, the burst release of TMZ from PCL-Diol-b-PU and gold-coated PCL-Diol-b-PU nanofibers were observed during the first 24 h (Stage I). The accumulation of TMZ on the surface of nanofibers could be responsible for the burst release of TMZ from nanofibers. The gradual higher burst release of TMZ from nanofibers with increasing TMZ content in nanofibers indicated the accumulation of higher drug molecules near or on the

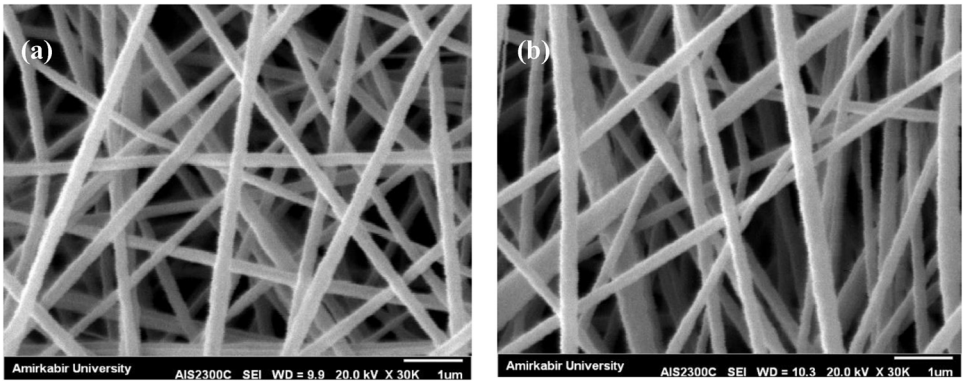

Fig. 6. SEM images of (a) pure PCL-Diol-b-PU nanofibers and (b) TMZ (40 mg) loaded PCL-Diol-b-PU nanofibers.

Table 1
Drug loading efficiency of nanofibrous formulations.

Formulation	TMZ content (mg)	Drug loading efficiency (%)
PCL-Diol-b-PU/TMZ nanofibers	10	95.2 ± 0.3
	20	95.1 ± 0.2
	40	94.8 ± 0.2
Gold-coated PCL-Diol-b-PU/TMZ nanofibers	10	72.3 ± 0.5
	20	70.5 ± 0.6
	40	66.1 ± 0.4

nanofibers surface [37]. The lower burst release rate of TMZ from gold-coated PCL-Diol-b-PU nanofibers compared to PCL-Diol-b-PU nanofibers could be due to the migration of TMZ molecules from the gold layer on the nanofiber surface to PBS solution and the lower drug content in gold coated TMZ loaded nanofibers. After that, the release rate was significantly decreased and the drug diffusion from the pores of nanofibers was a predominant reaction for further release of TMZ from nanofibers (Stage II). The drug release rate did not significantly change by increasing TMZ content at stage II. In stage (III), more time was needed for the TMZ molecules release from the fine pores of nanofibers. Therefore, the relatively small burst release and higher sustained release rate of TMZ from synthesized nanofibers can be achieved.

The Korsmeyer-Peppas release kinetic model is used to describe the TMZ release mechanism. The results are summarized in Table 2. As shown, for both nanofibrous formulations containing various TMZ contents, stage I of the release followed the non-Fickian diffusion. Therefore, TMZ molecules were released from the nanofibers surface and diffuse from the nanofibrous matrix at layers near the surface of nanofibers in stage I. In stages II and III, the TMZ release mechanism followed the Fickian diffusion which indicated that the diffusion of TMZ molecules from pores of nanofibers to the PBS solution was the predominant mechanism.

The calculated diffusion coefficients for stages II and III are summarized in Table 2. As shown, the diffusion coefficients in Stage III were lower than that of Stage II for all formulations. This behavior could be attributed to the diffusion of TMZ molecules from fine pores of nanofibers or diffusion of small molecules from pores of nanofibers which was slower than the diffusion of TMZ from nanofibers in stage II.

Fig. 9 shows the degradation behavior of PCL-Diol-b-PU/TMZ 20 mg nanofibers and gold-coated PCL-Diol-b-PU/TMZ 20 mg nanofibers during 5 weeks. As shown, there were a total of 7.5 ± 0.5 and 8.3 ± 0.2% mass loss of electrospun PCL-Diol-b-PU

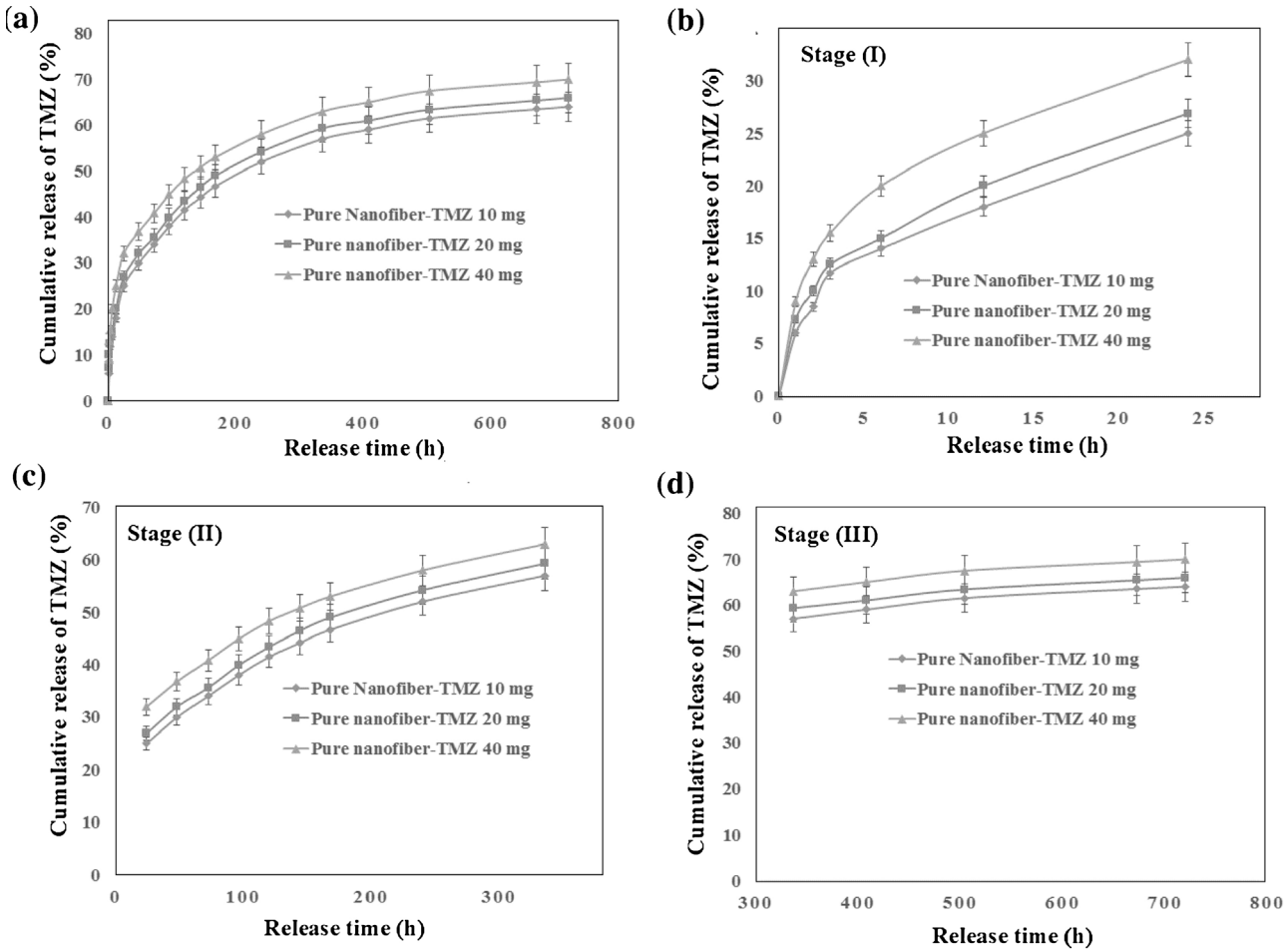

Fig. 7. (a) TMZ release from PCL-Diol-b-PU nanofibers, (b) Stage (I) of TMZ release profile during first 24 h, (c) Stage (II) of TMZ release profile from 24 h–14 days and (d) Stage (III) of TMZ release profile from 14days-30 days.

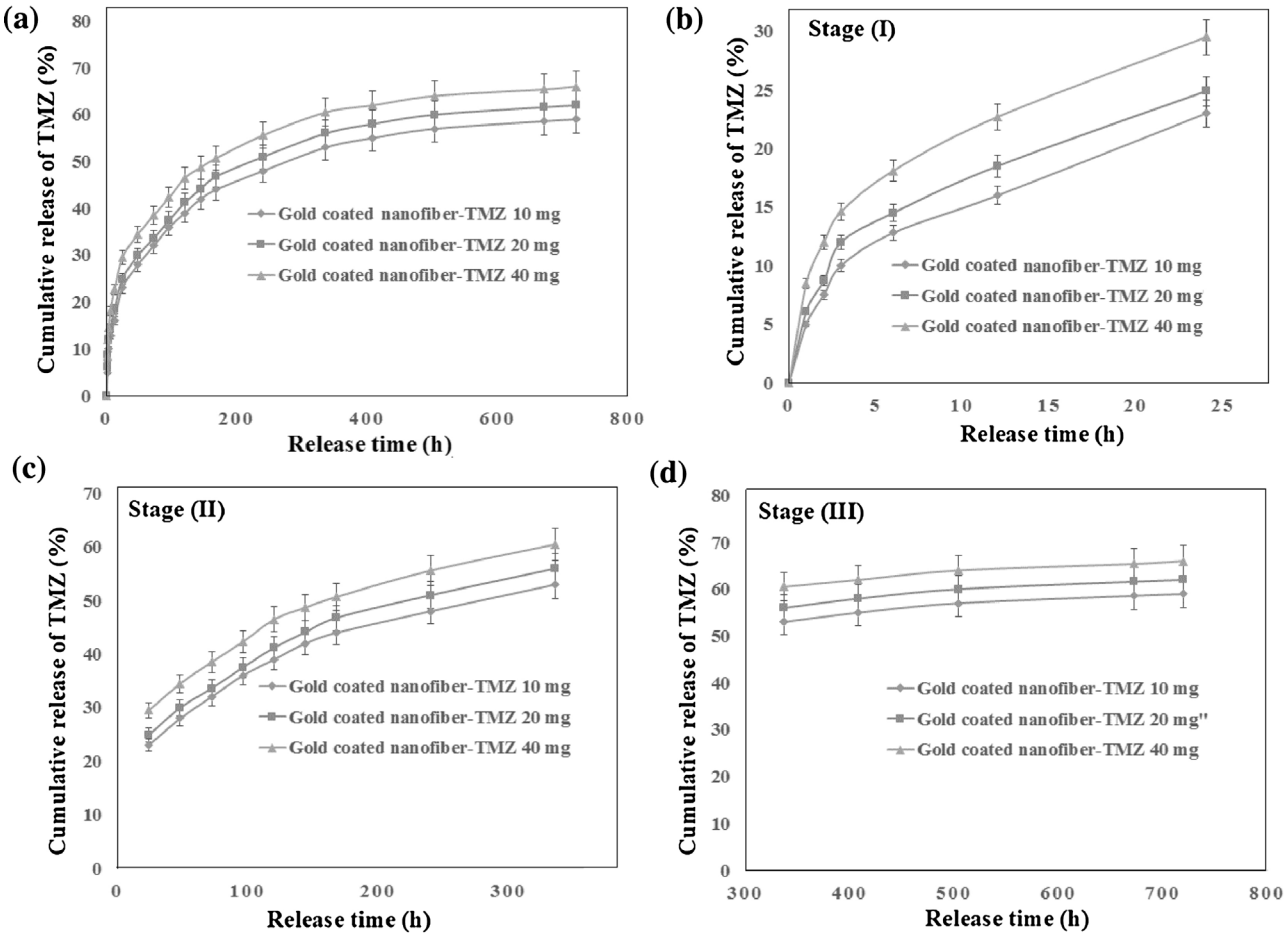

Fig. 8. (a) TMZ release from gold coated-PCL-Diol-b-PU nanofibers, (b) Stage (I) of TMZ release profile during first 24 h, (c) Stage (II) of TMZ release profile from 24 h–14 days and (d) Stage (III) of TMZ release profile from 14days-30 days.

Table 2
TMZ release kinetics and mechanisms for different stages of the TMZ release from nanofibers.

Formulation	TMZ (mg)	Stage	Model parameters		Release mechanism	Dapp $\times 10^{-17}$ (m^2/s)
			n	R^2		
Pure nanofiber	10	I	0.6025	0.988	1	–
		II	0.3529	0.992	2	5.087
		III	0.1501	0.981	2	0.948
Pure nanofiber	20	I	0.5840	0.991	1	–
		II	0.3153	0.994	2	5.552
		III	0.1396	0.991	2	0.960
Pure nanofiber	40	I	0.5810	0.986	1	–
		II	0.2995	0.993	2	6.489
		III	0.1326	0.985	2	0.972
Gold- nanofiber	10	I	0.6001	0.986	1	–
		II	0.3221	0.994	2	4.685
		III	0.1363	0.981	2	0.912
Gold- nanofiber	20	I	0.5833	0.985	1	–
		II	0.3126	0.992	2	4.998
		III	0.1294	0.978	2	0.930
Gold- nanofiber	40	I	0.5660	0.992	1	–
		II	0.2840	0.995	2	5.784
		III	0.1115	0.985	2	0.961

1: Non-Fickian diffusion, 2: Fickian diffusion.

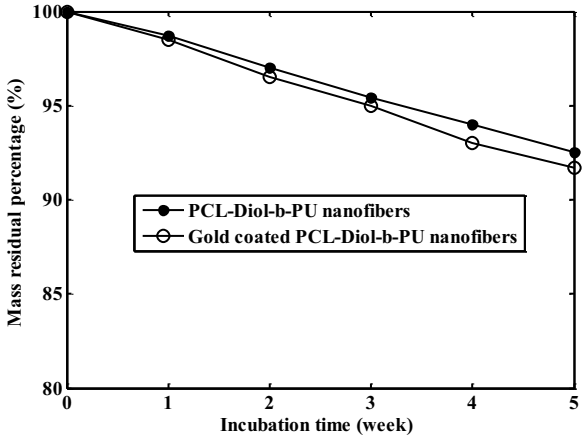

Fig. 9. Residual mass percentages of prepared nanofibers containing 20 mg TMZ.

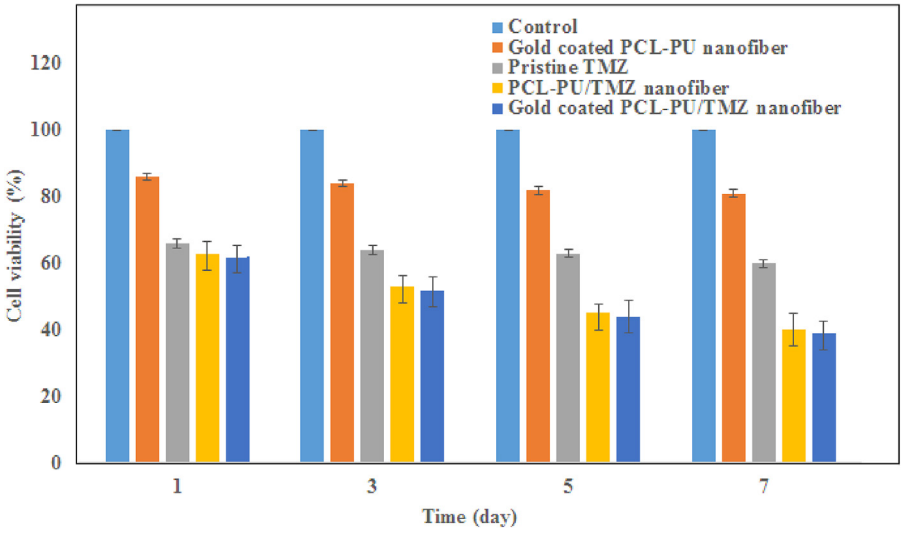

Fig. 10. In vitro cytotoxicity of TMZ, nanofiber/TMZ and gold coated nanofiber/TMZ against U-87 glioblastoma cells.

nanofibers and gold-coated PCL-Diol-b-PU nanofibers after 5 weeks incubation of nanofibers in PBS at 37 °C. This behavior indicated the high potential of synthesized nanofibers as a drug carrier.

3.5. Cell viability

The results of cell viability against U-87 human glioma cells are illustrated in Fig. 10. As shown, the viability of U-87 cells using pure TMZ was decreased to 66, 64, 63 and 60% after 1, 3, 5 and 7 days, respectively. There were no significant differences in cytotoxicity among glioma cells during 7 days using pure TMZ. The TMZ loaded PCL-Diol-b-PU nanofibers as well as TMZ loaded PCL-Diol-b-PU/gold nanofibers showed the higher cytotoxicity than the pure TMZ after 7 days. The viability of U-87 cells was significantly decreased after 1 day as a result of burst release. The more killing of U-87 cells within 7 days using TMZ loaded PCL-Diol-b-PU nanofibers and TMZ loaded PCL-Diol-b-PU/gold nanofibers could be attributed to the slower release of TMZ from nanofibers. The obtained results indicated the similar antitumor activities of both synthesized nanofibers against glioma cells within 7 days. As the TMZ content in the gold-coated PCL-Diol-b-PU nanofibers was lower than that of TMZ content in the PCL-Diol-b-PU nanofibers, the gold nanoparticles have a critical role in glioma cell killing. Therefore, the gold-coated PCL-Diol-b-PU nanofiber was more suitable for local delivery of TMZ from nanofibers.

4. Conclusion

In this work, the PCL-Diol-b-PU was successfully synthesized and the electrospinning process was used to fabricate nanofibers. The homogeneous PCL-Diol-b-PU nanofibers with average diameter of 235 nm were obtained under applied voltage of 19 kV, tip-collector distance of 12 cm, flow rate of 1 mL/h, the mixed solvent DMF/THF 8:2 and solution concentration of 10%. The TMZ chemotherapeutic drug has been loaded into the PCL-Diol-b-PU nanofibers. The uniform gold nanoparticles with average particle size of 18 nm were successfully synthesized and coated on the nanofibers surface. The high TMZ encapsulation efficiency of fabricated nanofibers was observed. Both PCL-Diol-b-PU and gold-coated PCL-Diol-b-PU nanofibers exhibited the sustained TMZ release for more than 30 days with low burst release. The “n “values of Korsmeyer-Peppas indicated the non-Fickian diffusion mechanism within the first 24 h and after that the Fickian diffusion mechanism during the sustained TMZ release over 30 days. The cytotoxicity of PCL-Diol-b-PU/TMZ nanofibers was enhanced by gold coating on the nanofibers surface. The results revealed that the gold-coated PCL-Diol-b-PU nanofibers can be used as suitable

drug delivery implants to deliver TMZ against glioma brain tumors, successfully.

Acknowledgement

This work was supported by grant from the Amirkabir University of Technology of Iran.

References

[1] M.S. Lesniak, H. Brem, Targeted therapy for brain tumors, Nat. Rev. 3 (2004) 499–508.
[2] J. Xie, C.H. Wang, Electrospun micro and nanofibers for sustained delivery of paclitaxel to treat C6 glioma in vitro, Pharm. Res. 23 (2006) 1817–1826.
[3] B. Wang, H. Li, Q. Yao, Y. Zhang, X. Zhu, T. Xia, J. Wang, G. Li, X. Li, S. Ni, Local in vitro delivery of rapamycin from electrospun PEO/PDLLA nanofibers for glioblastoma treatment, Biomed. Pharmacother. 83 (2016) 1345–1352.
[4] B. Ardeshirzadeh, N. Aboutalebi Anaraki, M. Irani, L. Roshanfekr Rad, S. Shamshiri, Controlled release of doxorubicin from electrospun PEO/chitosan/graphene oxide nanocomposite nanofibrous scaffolds, Mater. Sci. Eng. C 48 (2015) 384–390.
[5] M. Chen, W. Feng, S. Lin, C. He, Y. Gao, H. Wang, Antitumor efficacy of a PLGA composite nanofiber embedded with doxorubicin@MSNs and hydroxycamptothecin@HANPs, RSC Adv. 4 (2014) 53344–53351.
[6] S. Ni, X. Fan, J. Wang, H. Qi, X. Li, Biodegradable implants efficiently deliver combination of paclitaxel and temozolomide to glioma C6 cancer cells in vitro, Ann. Biomed. Eng. 42 (2014) 214–221.
[7] L. Hosseini, K. Mahboobnia, M. Irani, Fabrication of PLA/MWCNT/Fe_3O_4 composite nanofibers for leukemia cancer cells, Int. J. Polym. Mater. 65 (2016) 176–182.
[8] N. Aboutalebi Anaraki, L. Roshanfekr Rad, M. Irani, I. Haririan, Fabrication of PLA/PEG/MWCNT electrospun nanofibrous scaffolds for anticancer drug delivery, J. Appl. Polym. Sci. 132 (2014) 1–9.
[9] S. Liu, G. Zhou, D. Liu, Z. Xie, Y. Huang, X. Wang, W. Wud, X. Jing, Inhibition of ortho-topic secondary hepatic carcinoma in mice by doxorubicin-loaded electrospun polylactide nanofibers, J. Mater. Chem. B 1 (2013) 101–109.
[10] D. Liu, S. Liu, X. Jing, X. Li, W. Li, Y. Huang, Necrosis of cervical carcinoma by dichloroacetate released from electrospun polylactide mats, Biomaterials 33 (2012) 4362–4369.
[11] K. Qiu, C. He, W. Feng, W. Wang, X. Zhou, Z. Yin, L. Chen, H. Wang, X. Mo, Doxorubicin-loaded electrospun poly(L-lactic acid)/mesoporous silica nanoparticles composite nanofibers for potential postsurgical cancer treatment, J. Mater. Chem. B 1 (2013) 4601–4611.
[12] M. Song, C. Pan, C. Chen, J. Li, X. Wang, Z. Gu, The application of new nanocomposites: enhancement effect of polylactide nanofibers/nano-TiO_2 blends on biorecognition of anticancer drug daunorubicin, Appl. Surf. Sci. 255 (2008) 610–612.
[13] J. Li, C. Chen, X. Wang, Z. Gu, B. Chen, Novel strategy to fabricate PLA/Au nanocomposites as an efficient drug carrier for human leukemia cells in vitro, Nanoscale Res. Lett. 6 (29) (2011) 1–8.
[14] X. Xu, X. Chen, Z. Wang, X. Jing, Ultrafine PEG–PLA fibers loaded with both paclitaxel and doxorubicin hydrochloride and their in vitro cytotoxicity, Eur. J. Pharm. Biopharm. 72 (2009) 18–25.
[15] S.Y. Kim, M. Kim, M.K. Kim, H. Lee, D.K. Lee, D.H. Lee, S.G. Yang, Paclitaxel-eluting nanofiber-covered self-expanding nonvascular stent for palliative chemotherapy of gastrointestinal cancer and its related stenosis, Biomed. Microdev. 16 (2014) 897–904.
[16] J. Xie, R.S. Tan, C.H. Wang, Biodegradable microparticles and fiber fabrics for sustained delivery of cisplatin to treat C6 glioma in vitro, J. Biomed. Mater. Res. A 85 (2008) 897–908.
[17] S.H. Ranganath, C.H. Wang, Biodegradable microfiber implants delivering paclitaxel for post-surgical chemotherapy against malignant glioma, Biomaterials 29 (2008) 2996–3003.
[18] S.S. Rao, M.T. Nelson, R. Xue, J.K. De Jesus, M.S. Viapiano, J.J. Lannutti, A. Sarkar, J.O. Winter, Mimicking white matter tract topography using core-shell electrospun nanofibers to examine migration of malignant brain tumors, Biomaterials 34 (2013) 5181–5190.
[19] G. Guo, S.Z. Fu, L.X. Zhou, H. Liang, M. Fan, F. Luo, Z.Y. Qian, Y.Q. Wei, Preparation of curcumin loaded poly(ε-caprolactone)-poly(ethylene glycol)-poly(ε-caprolactone) nanofibers and their in vitro antitumor activity against Glioma 9L cells, Nanoscale 3 (2011) 3825–3832.
[20] T.T. Reddy, M. Hadano, A. Takahara, Controlled release of model drug from biodegradable segmented polyurethane ureas: morphological and structural features, Macromol. Symp. 242 (2006) 241–249.
[21] A. Omuro, Glioblastoma and other malignant gliomas, JAMA J. Am. Med. Assoc. 310 (2013) 1842–1850.
[22] A. Di Martino, A. Pavelkova, S. Maciulyte, S. Budriene, V. Sedlarik, Polysaccharide-based nanocomplexes for co-encapsulation and controlled release of 5-Fluorouracil and Temozolomide, Eur. J. Pharm. Sci. 92 (2016) 276–286.
[23] C. Fang, K. Wang, Z.R. Stephen, Q. Mu, F.M. Kievit, D.T. Chiu, O.W. Press, M. Zhang, Temozolomide nanoparticles for targeted glioblastoma therapy, ACS Appl. Mater. Interfaces 7 (2015) 6674–6682.
[24] A. Di Martino, V. Sedlarik, Amphiphilic chitosan-grafted-functionalized polylactic acid based nanoparticles as a delivery system for doxorubicin and temozolomideco-therapy, Int. J. Pharm. 20 (2014) 134–145.
[25] S. Huo, H. Ma, K. Huang, J. Liu, T. Wei, S. Jin, J. Zhang, S. He1, X.J. Liang, Superior penetration and retention behavior of 50 nm gold nanoparticles in tumors, Cancer Res. 73 (2012) 319–330.
[26] D.Y. Joh, L. Sun, M. Stang, A.A. Zaki, S. Murty, P.P. Santoiemma, J.J. Davis, B.C. Baumann, M.A. Basanta, D. Bhang, G.D. Kao, A. Tsourkas, J.F. Dorse, Selective targeting of brain tumors with gold nanoparticle-induced radio sensitization, PLoS One 8 (62425) (2013) 1–10.
[27] S. Dhar, E.M. Reddy, A. Shiras, V. Pokharkar, B.L.V. Prasad, Natural gum reduced/stabilized gold nanoparticles for drug delivery formulations, Chem. Eur. J. 14 (2008) 10244–10250.
[28] M. Haghayegh, G. Mir Mohamad Sadeghi, Synthesis of shape memory polyurethane/clay nanocomposites and analysis of shape memory, thermal, and mechanical properties, Polym. Compos. 33 (2012) 843–849.
[29] R. Levy, N.T.K. Thanh, R.C. Doty, I. Hussain, R.J. Nichols, D.J. Schiffrin, M. Brust, D. G. Fernig, Rational and combinatorial design of peptide capping ligands for gold nanoparticles, J. Am. Chem. Soc. 126 (2004) 10076–10084.
[30] P. Costa, J. Manuel, Modeling and comparison of dissolution profiles, Eur. J. Pharm. Sci. 13 (2001) 123–133.
[31] R. Salehi, M. Irani, M.R. Rashidi, A. Aroujalian, A. Raisi, M. Eskandani, I. Haririan, S. Davaran, Stimuli-responsive nanofibers prepared from poly (Nisopropylacrylamide–acrylamide–vinyl pyrrolidone) by electrospinning as an anticancer drug delivery, Des. Monom. Polym. 16 (2013) 515–527.
[32] R. Salehi, M. Irani, M.-R. Rashidi, K. Nowruzi, M. Eskandani, I. Haririan, S. Davaran, Interaction, controlled release, and antitumor activity of doxorubicin hydrochloride from pH-sensitive P(NIPAAm-MAA-VP) nanofibrous scaffolds prepared by green electrospinning, Int. J. Polym. Mater. 63 (2014) 609–619.
[33] X.H. Tian, X.N. Lin, F. Wei, W. Feng, Z.C. Huang, P. Wang, L. Ren, Y. Diao, Enhanced brain targeting of temozolomidein polysorbate-80 coated polybutylcyanoacrylate nanoparticles, Int. J. Nanomed. 6 (2011) 445–452.
[34] A. Orza, O. Soritau, L. Olenic, M. Diudea, A. Florea, D.R. Ciuca, C. Mihu, D. Casciano, A.S. Biris, Electrically conductive gold-coated collagen nanofibers for placental- derived mesenchymal stem cells enhanced differentiation and proliferation, ACS Nano 5 (2011) 4490–4503.
[35] R. Erdem, İ. Usta, M. Akalin, O. Atak, M. Yuksek, A. Pars, The impact of solvent type and mixing ratios of solvents on the properties of polyurethane based electrospun nanofibers, Appl. Surf. Sci. 334 (2015) 227–230.
[36] H. Zhuo, J. Hu, S. Chen, L. Yeung, Preparation of polyurethane nanofibers by electrospinning, J. Appl. Polym. Sci 109 (2008) 406–411.
[37] A. Sohrabi, P.M. Shaibani, H. Etayash, K. Kaur, T. Thundat, Sustained drug release and antibacterial activity of ampicillin incorporated poly(methyl methacrylate)enylon6 core/shell nanofibers, Polymer 54 (2013) 2699–2705.